A new ALE formulation for sloshing analysis

N. Aquelet† and M. Souli‡

Université de Lille, Laboratoire de Mécanique de Lille, CNRS 1441,
Bd Paul Langevin Villeneuve d'Ascq, France

J. Gabrys‡†

The Boeing Company, Rotorcraft Division, Philadelphia, PA, USA

L. Olovson‡†

L.S.T.C., Livermore Software Technology Corporation, Livermore, California, USA

Abstract. Arbitrary Lagrangian Eulerian finite element methods gain interest for the capability to control mesh geometry independently from material geometry, the ALE methods are used to create a new undistorted mesh for the fluid domain. In this paper we use the ALE technique to solve fuel slosh problem. Fuel slosh is an important design consideration not only for the fuel tank, but also for the structure supporting the fuel tank. "Fuel slosh" can be generated by many ways: abrupt changes in acceleration (braking), as well as abrupt changes in direction (highway exit-ramp). Repetitive motion can also be involved if a "sloshing resonance" is generated. These sloshing events can in turn affect the overall performance of the parent structure. A finite element analysis method has been developed to analyze this complex event. A new ALE formulation for the fluid mesh has been developed to keep the fluid mesh integrity during the motion of the tank. This paper explains the analysis capabilities on a technical level. Following the explanation, the analysis capabilities are validated against theoretical using potential flow for calculating fuel slosh frequency.

Key words: ALE; sloshing; multi-material formulation.

1. Introduction

The Arbitrary Lagrangian Eulerian (ALE) approach is based on the arbitrary movement of a reference domain which, additionally to the common material domain and spatial domain, is introduced as a third domain, as detailed in (Hughes *et al.* 1981). In this reference domain, which will later on correspond to the finite element mesh, the problem is formulated. The arbitrary movement of the reference frame, accompanied of course by a good "mesh moving algorithm",

---

† Graduate Student

‡ Professor

‡† Senior Research Scientist

enables us to rather conveniently deal with moving boundaries, free surfaces, large deformations, and interface contact problems. Sloshing tank is a typical example for free surface problems in industrial application and academia. In sloshing tank problems, when the tank is partially filled, both gas and liquid coexist and the interface between these two phases is called a "free surface". The "free surface" designation means that the interface is not constrained by the gas. In other words, the difference between the liquid and gas densities is such that the only influence of the gas on the liquid surface is a relatively low pressure. Under these conditions, if the tank moves abruptly, a physical phenomenon occurs called 'sloshing'.

The definition of fuel slosh is the following "Liquid fuels are violently turbulent in the fuel cell during hard acceleration, cornering, braking, and from rough terrain" (Summit Racing Equipment). The effect of this fluid sloshing concerns both tank designers and Classification Societies. To summarize, there are three distinct areas of concern:

1. *Sloshing loads on the tank itself.* This is concerned with the tank fracturing during operation. One example deals with the Coast Guard. The Code of Federal Regulations defines a required slosh test for fuel tanks on all boats and associated equipment.
2. *Sloshing loads on the parent structure.* Slosh loads can have serious effects on the performance of the parent structure. For example, the sloshing of a partially filled tank can jeopardize the rollover stability of a tanker truck.
3. *Sloshing and tank usefulness.* The sloshing event may inhibit the effectiveness of pumps/gauges within the tank. For example, during a sloshing event, a fuel pump may not be able to pump fuel.

The traditional method for analyzing fuel slosh was with a simple hand calculation (Blevins 1995). However, this method is limited to gentle sloshing - no slosh contacting the tank lid, rigid tank walls, rigid baffles without hole (Lee *et al.* 2002), etc. Thus, to predict accurately the sloshing phenomenon, numerical techniques, which correctly model the free surface, were required. These numerical solution algorithms have been developed for both the Lagrangian formulation and the Eulerian formulation. In general, the choice of which representation to use depends on the characteristics of the specific problem. For example, when the free surface undergoes large deformations, the Lagrangian formulation is not well suited and the Eulerian formulation is chosen. Regardless of the formulation employed, this paper will briefly review the numerical approaches that have been used to track the free surface. In particular, the ALE formulation, with an interface tracking method, will be discussed.

The outline of this paper is arranged as follows. In section 2, a general description of the Lagrangian phase and ALE formulation are described. Section 3 discusses the advection algorithms used to solve conservation of mass, momentum and internal energy. Section 4 is devoted to interface tracking. Specifically, the interface tracking method developed by Young (1982), and adapted to our problem, is described. The last sections, 5 and 6, will both demonstrate the capabilities of the analysis code by comparing predicted sloshing frequencies with formula calculated sloshing frequencies.

2. ALE and VOF formulation

Fluid problems, in which interfaces between different materials (fuel and air, or fuel and void) are present, are more easily modelled by using a Lagrangian mesh. However, if an analysis for complex

tank geometry is required, the distortion of the Lagrangian mesh makes such a method difficult to use many re-meshing steps are necessary for the calculation to continue. Another method to use is the Eulerian formulation. This change from a Lagrangian to an Eulerian formulation, however, introduces two problems. The first problem is the interface tracking (Nakayama and Mori 1996) and the second problem is the advection phase or advection of fluid material across element boundaries.

To solve these problems, an explicit finite element method for the Lagrangian phase and a finite volume method (flux method) for the advection phase are used. We can refer to several explicit codes such as Pronto, Dyna3D and LS-DYNA; see (Hallquist 1998) for a full description of the explicit finite element method.

The advection phase has been added to the LS-DYNA code extending the range of applications that can be used with the ALE formulation (Souli and Zolesio 2001). Current applications include sloshing involving a 'free surface', and high velocity impact problems where the target is modeled as a fluid material, thus providing a more realistic representation of the impact event by capturing large deformations.

An ALE formulation contains both pure Lagrangian and pure Eulerian formulations. The pure Lagrangian description is the approach that: the mesh moves with the material, making it easy to track interfaces and to apply boundary conditions. Using an Eulerian description, the mesh remains fixed while the material passes through it. Interfaces and boundary conditions are difficult to track using this approach; however, mesh distortion is not a problem because the mesh never changes. In solid mechanics a pure Eulerian formulation it is not useful because it can handle only a single material in an element, while an ALE formulation is assumed to be capable of handling more than one material in an element.

In the ALE description, an arbitrary referential coordinate is introduced in addition to the Lagrangian and Eulerian coordinates. The material derivative with respect to the reference coordinate can be described as (1). Thus substituting the relationship between the material time derivative and the reference configuration time derivative derives the ALE equations,

$$\frac{\partial f(X_i, t)}{\partial t} = \frac{\partial f(x_i, t)}{\partial t} + w_i \frac{\partial f(x_i, t)}{\partial x_i} \tag{1}$$

where X_i is the Lagrangian coordinate, x_i the Eulerian coordinate, w_i is the relative velocity. Let denote by v the velocity of the material and by u the velocity of the mesh. In order to simplify the equations we introduce the relative velocity $w = v - u$. Thus the governing equations for the ALE formulation are given by the following conservation equations:

(i) Mass equation.

$$\frac{\partial \rho}{\partial t} = -\rho \frac{\partial v_i}{\partial x_i} - w_i \frac{\partial \rho}{\partial x_i} \tag{2}$$

(ii) Momentum equation.

The strong form of the problem governing Newtonian fluid flow in a fixed domain consists of the governing equations and suitable initial and boundary conditions. The equations governing the fluid problem are the ALE description of the Navier-Stokes equations:

$$\rho \frac{\partial v_i}{\partial t} = \sigma_{ij,j} + \rho b_i - \rho w_i \frac{\partial v_i}{\partial x_j} \tag{3}$$

The stress tensor σ_{ij} is described as follows:

$$\sigma_{ij} = -p\,\delta_{ij} + \mu(v_{i,j} + v_{j,i}).$$

The last equations are solved with the following boundary conditions and initial conditions:

$$v_i = U_i^0 \quad \text{on} \quad \Gamma_1 \tag{4}$$

$$\sigma_{ij}n_j = 0 \quad \text{on} \quad \Gamma_2 \tag{5}$$

where

$$\Gamma_1 \cup \Gamma_2 = \Gamma, \qquad \Gamma_1 \cap \Gamma_2 = 0 \tag{6}$$

Γ is the whole boundary of the calculation domain, and Γ_1 and Γ_2 are partial boundaries of Γ. The superscript means prescribed value, n_i is the outward unit normal vector on the boundary, and δ_{ij} is Kronecker's delta function. The velocity field is assumed as known at $t = 0$ in the whole domain Ω.

$$v_i(x_i, 0) = 0 \tag{7}$$

(iii) Energy equation.

$$\rho \frac{\partial E}{\partial t} = \sigma_{ij}v_{i,j} + \rho b_i v_i - \rho w_j \frac{\partial E}{\partial x_j} \tag{8}$$

Note that the Eulerian equations are derived by assuming that the velocity of the reference configuration is zero and that the relative velocity between the material and the reference configuration is therefore the material velocity. The term in the relative velocity in (3) and (4) is usually referred to as the advective term, and accounts for the transport of the material past the mesh. It is the additional term in the equations that makes solving the ALE equations much more difficult numerically than the Lagrangian equations, where the relative velocity is zero.

There are two ways to implement the ALE equations, and they correspond to the two approaches taken in implementing the Eulerian viewpoint in fluid mechanics. The first way solves the fully coupled equations for computational fluid mechanics; this approach used by different authors can handle only a single material in an element. The alternative approach is referred to as an operator split in the literature, where the calculation, for each time step is divided into two phases. First a Lagrangian phase is performed, in which the mesh moves with the material, in this phase the changes in velocity an internal energy due to the internal and external forces are calculated. The equilibrium equations are:

$$\rho \frac{\partial v_i}{\partial t} = \sigma_{ij,j} + \rho b_i, \tag{9}$$

$$\rho \frac{\partial E}{\partial t} = \sigma_{ij}v_{i,j} + \rho b_i v_i. \tag{10}$$

In the Lagrangian phase, mass is automatically conserved, since no material flows across the element boundaries.

In the second phase, the advection phase, transport of mass, internal energy and momentum across cell boundaries are computed; this may be thought of as remapping the displaced mesh at the Lagrangian phase back to its original or arbitrary position.

From a discretization point of view of (9) and (10), one point integration is used for efficiency and to eliminate locking, Benson (1997). The zero energy modes are controlled with an hourglass viscosity (Flanagan and Belytschko 1981). A shock viscosity, with linear and quadratic terms, is used to resolve the shock wave (Richtmyer and Morton 1967); a pressure term is added to the pressure in the energy Eq. (10). The resolution is advanced in time with the central difference method, which provides a second order accuracy in time using an explicit method in time.

For each node, the velocity and displacement are updated as follows:

$$u^{n+1/2} = u^{n-1/2} + \Delta t \cdot M^{-1} \cdot (F_{exl} + F_{int})$$

$$x^{n+1} = x^{n-1} + \Delta t u^{n+1/2} \tag{11}$$

Where F_{int} is the internal vector force and F_{ext} the external vector force associated with body forces and boundary conditions, M is the mass matrix diagonalized. For each element of the mesh, the internal force is computed as follows:

$$F_{int} = \sum_{k=1}^{Nelem} \int_k B^t \cdot \sigma \cdot dv$$

B is the gradient matrix and *Nelem* is the number of elements.

The time step size, Δt, is limited by the Courant stability condition (Hallquist 1998), which may be expressed as:

$$\Delta t \leq \frac{l}{Q + (Q^2 + c^2)^{1/2}} \tag{12}$$

$$Q = C_1 \cdot c + C_2 |div(u)| \quad \text{for} \quad div(u) < 0$$

$$Q = 0 \qquad\qquad\qquad div(u) \geq 0$$

Where l is the characteristic length of the element, Q is a term derived from the shock viscosity, C_1 and C_2 are the coefficients for the linear and quadratic terms of the shock viscosity. The Q term introduced in the equation is positive for compression and zero for tension, when c is the speed of sound through the material in the element. For a solid material, the speed of sound is:

$$c^2 = \frac{\frac{4}{3}G + k}{\rho_0} \tag{13}$$

$$k = \rho_0 \frac{\partial P}{\partial \rho} + \frac{P}{\rho} \frac{\partial P}{\partial e} \tag{14}$$

where ρ is the material density, G is the shear modulus, and $P(\rho, e)$ is the equation of state. In (14), the second term on the right hand side accounts for the stiffening effect due to the increase of internal energy as the material is compressed. For a fluid material, $k = \rho_0 c^2$ in which ρ_0 is the mass density and c is the sound velocity. For fluid material the viscosity is ignored in the calculation of the speed of sound. For sloshing tank problems the pressure is much greater than the deviatoric components stress due the fluid viscosity, and the deviatoric stress is sometimes ignored.

The VOF (Volume of Fluid) method is attractive for solving a broad range of non-linear problems in fluid and solid mechanics, because it allows arbitrary large deformations and enables free surfaces to evolve. The Lagrangian phase of the VOF method is easily implemented in an explicit ALE finite element method. Before advection, special treatment for the partially voided element is needed. For an element that is partially filled, the volume fraction satisfies

$$V_f \leq 1 \tag{15}$$

The total stress by σ is weighed by volume fraction.

$$\sigma_f = \sigma \cdot V_f \tag{16}$$

For voided elements, the stress is zero. In the computational process, the elements loop goes only through elements that are not voided. For free surface problems, the elements that are partially filled $(V_f < 1)$ define the free surface. In order to compute accurately the free surface in a sloshing problem, interface-tracking algorithm is performed before the remesh process and advection phase.

3. Moving mesh algorithm

The remeshing process is needed for some sloshing problems. However, for arbitrary moving tanks, the fluid mesh moves as a rigid mesh following the tank. This new ALE feature allows the mesh to stay regular, and the time step, which can be affected by mesh distortion, to be stable. In other words, there is only mesh motion and no mesh distortion due to the ALE formulation. This method is very useful for moving or rotating tanks (see Fig. 1), where the fluid mesh will move and rotate with the tank without undergoing any mesh deformation.
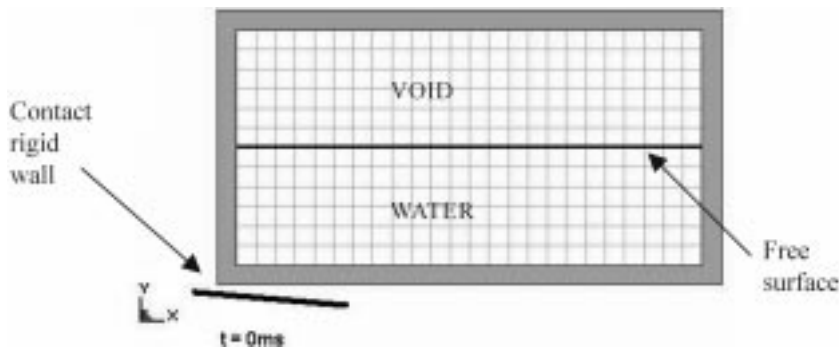

Fig. 1 Free drop test on an inclined rigid plate

Fig. 1 describes a drop test of a partially filled rigid structure tank on an inclined rigid plate. The new ALE algorithm allows the fluid mesh to follow the movement of the structure. The integrity of mesh structure is maintained. As the structure impacts the rigid plate and then moves and rotates, the fluid mesh moves as a rigid mesh in the coordinate system attached to the structure. This ALE algorithm can be applied to several problems in moving structure that are rigid or undergo small deformations. The following Fig. 2 describes the location of the tank at time $t = 0$ ms, $t = 19$ ms, $t = 38$ ms and $t = 58$ ms as well as the free surface separating the fluid material and the void.

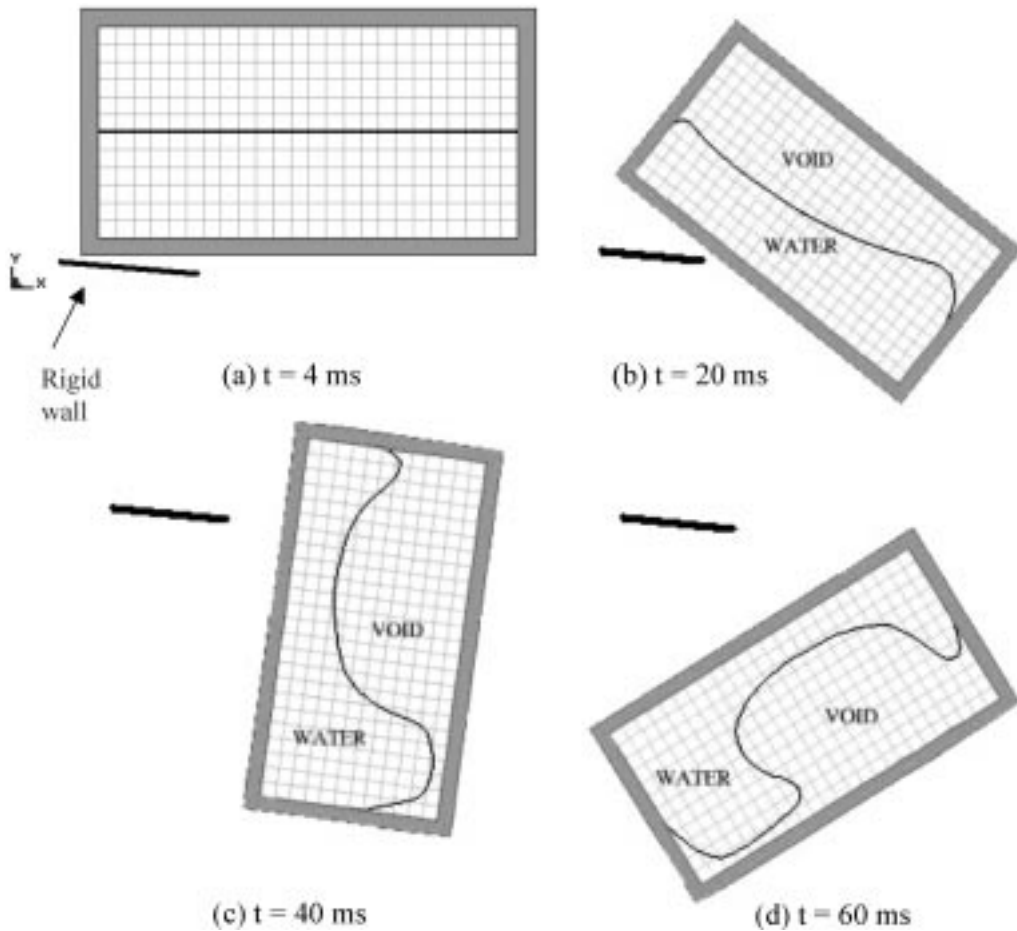(a) t = 4 ms   (b) t = 20 ms

(c) t = 40 ms   (d) t = 60 ms

Fig. 2 Free drop test, and free surface location

Different ALE formulations can be used if the tank is not rigid, and may undergo large deformations. For these applications, a fluid structure coupling needs to be performed to take into account the structure deformations as well as these effects on the fluid. The goal of this paper is to focus on the sloshing problem for rigid tanks. Fluid structure coupling for compliant structure requires more sophisticated ALE algorithms that we will present in a following paper.

4. Stress equilibrium and interface tracking

After the Lagrangian phase is performed, either the stress tensor, pressure and deviatoric stress should be equilibrated, but most mixture theories equilibrate only pressure, Benson (1997), the pressure equilibrium is a non-linear problem, which is complex and expensive to solve. Skipping the stress equilibrium phase is assuming an equal strain rate for both materials, which is incorrect. For most problems, the linear distribution based on volume fraction of the volumetric strain during the Lagrangian phase also leads to incorrect results. The volume distribution should be scaled by the bulk compression of the two materials in the element. For example, in an element containing air and water, the air, which is highly compressible, will absorb most of the volumetric strain. By assuming an equal strain rate or volumetric strain scaled on the volume fraction of the element, the water is forced to accept the same amount of strain as the air, and will undergo artificial high stresses.

There are several methods to treat the free surface in a fluid problem; the common one is the MAC method, which involves Eulerian flow calculation and Lagrangian particle movement. The velocity of the markers is found first by locating the fluid cell containing the particle and taking the average velocities of the cell nodes (the average is based on the finite element particles in the fluid cell). The particle cells have small inertia and tend to follow the fluid flow. However, the MAC method becomes complicated if the interfaces become highly distorted or if the geometry is complex.

Another possible way of tracking interfaces is the use of the volume fractions of the elements, or the Young method (Young 1982). The Young method is developed to track an interface in elements containing two materials for two-dimensional problems. This method is adapted in this paper for the two dimensional problems. In this method, the material layout is described solely by the volume fraction of the fluid material in the element. Specifically, a straight line using the SLIC technique (Simple Linear Interface Calculation) of Woodward and Collela (1982) approximates the interface in the cell. Interfaces are initially drawn parallel to the element faces. Then nodal volume fraction is computed to each node based on the fraction volumes of elements that share the same node. This volume fraction determines the slope of the material interface inside the element. The position of the interface (see Fig. 3) is then adjusted so that it divides the element into two volumes, which correctly matches the element volume fraction.

The interface position is used to calculate the volume of the fluid flowing across cell sides. The normal vector to the interface inside the element is defined by:

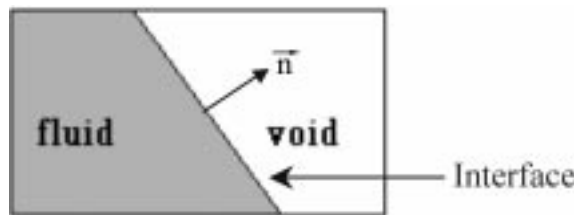$$\vec{n} = \frac{\overrightarrow{grad f}}{\left|\overrightarrow{grad f}\right|}$$

Fig. 3 Interface between two materials, air and water, is oriented by the normal $\vec{n}$ in a Eulerian cell

where f is the nodal volume fraction. As the X-advection, Y-advection and Z-advection are calculated in separate steps, it is sufficient to consider the flow across one side only. The interface calculation prevents advection of very small fluxes between partially filled and empty elements. Instead fluid flow is transported from 'filled' element to 'empty' element and this change in volume will be monitored and used to 'fill-up' the element or increase its volume fraction.

5. Advection phase

In the second phase, the transport of mass, momentum and internal energy across the element boundaries is computed. This phase may be considered as a 're-mapping' phase. The displaced mesh from the Lagrangian phase is remapped into the initial mesh for an Eulerian formulation, or an arbitrary distorted mesh for an ALE formulation.

In this advection phase, we solve a hyperbolic problem, or a transport problem, where the variables are density, momentum per unit volume and internal energy per unit volume. Details of the numerical method used to solve the equations are described in detail in (Young 1982, Benson 1992), where the Donor Cell algorithm, a first order advection method and the Van Leer algorithm, a second order advection method (Van Leer 1977) are used. As an example, the equation for mass conservation is:

$$\frac{\partial \rho}{\partial t} + \nabla \cdot (\rho u) = 0 \qquad (17)$$

It is not the goal of this paper to describe the different algorithms used to solve the Eq. (17); these algorithms have already been described in detail by Benson (1992) and Souli *et al.* (2000). In this section, we will focus on the 'staggered' mesh used for the momentum advection, Benson (1992).

The advected momentum is used for the computation of the new nodal velocities. To prevent distribution of momentum from nodes to elements during the advection and from elements to nodes during nodal velocity calculations, the momentum advection is done only through the nodes. This procedure requires a staggered mesh. A mesh is staggered with respect to the original mesh so that the original mesh centroids become the new nodes. Yaqui (Amsden and Hirt 1973) developed the first code to construct a staggered mesh (see Fig. 4) for the momentum advection, and the basic idea is still in common use.
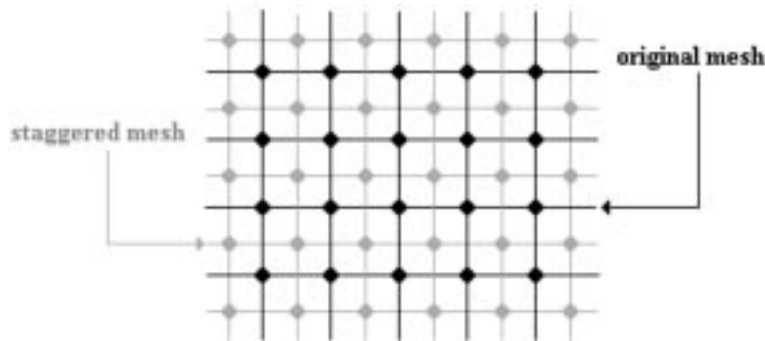
Fig. 4 Staggered mesh and original mesh

A cell centred advection algorithm is applied to the staggered mesh for the momentum advection. The data necessary for the advection algorithm are the cell volume before and after the Lagrangian phase, nodal velocities, nodal masses and fluxes between cells. All the data are ready on the staggered mesh except for the fluxes. The new flux values on the staggered mesh are defined using a regular distribution of the fluxes from the original mesh element faces to the new element faces. Once the new flux on the staggered mesh is computed, the momentum advection is performed according to the following algorithm:

$$V^+ M^+ = V^- M^- + \sum_{j=1}^{Nbedges} V_j^- M_j^- \tag{18}$$

where the superscripts '−' and '+' refer to the solution values before and after the transport. Values that are subscripted by j refer to the boundaries of the elements, through which the material flow, and the V_j^- are the fluxes transported through the adjacent elements, these fluxes are computed using the staggered mesh. The flux is positive if the element received material and negative if the element is loosing material. Details of the advection algorithm are described in (Benson 1998).

6. Analytical model

The fluid motions of a partially filled tank are studied using a bidimensional mathematical model. The liquid in an open tank (see Fig. 5) can flow back and forth across the basin in standing waves at discrete natural frequencies. The purpose of this section is to find the natural frequency and mode shape of a two-dimensional partially filled tank by using Fourier Series expansion. The liquid is assumed homogeneous, inviscid, irrotational and incompressible. The boundaries are rigid: the fluctuations in pressure on the walls due to sloshing exclude flexing of the tank wall that can have a significant influence on the natural frequencies and mode shapes of sloshing in extreme case. Non-linear effects are neglected: the wave amplitudes are very small in comparison with the wavelengths and depths. Po represents the pressure of the surrounding atmosphere and the surface tension is negligible.

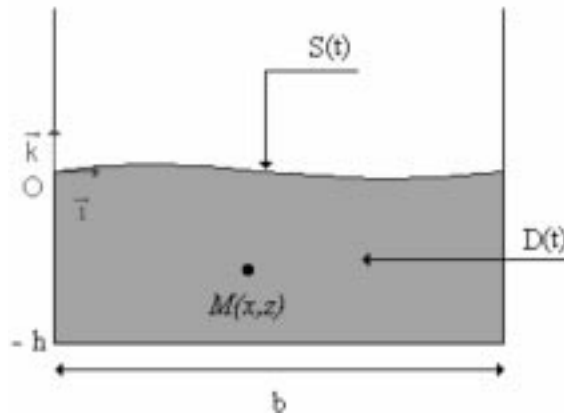The fluid of Fig. 5 represents the domain called $D(t)$ and the free surface, which separates the

Fig. 5 Partially filled tank

fluid material from the atmosphere, is the boundary called $S(t)$.

A particle $M(x, z)$ is represented by its location in the (x, z) plane, $\overrightarrow{OM} = x \cdot \vec{i} + z \cdot \vec{k}$ in the plan $(O, \vec{i}, \vec{k})$. The fluid particle velocity is defined by:

$$\vec{V}(x, z, t) = \frac{d\overrightarrow{OM}(x, z, t)}{dt}$$

where d/dt is the particle derivative.

A very small perturbation of the free surface is assumed. Therefore, in the general asymptotic expansion of any physical variable (see Eq. (19)), in which epsilon ε is considered as a small parameter, the approximation is carried out to the first order. Higher order terms than ε are neglected in the following asymptotic expansion:

$$\lambda = \lambda^{(o)} + \varepsilon \cdot \lambda^{(1)} + O(\varepsilon) \tag{19}$$

Since the fluid is assumed incompressible, non-rotational and inviscid, the Eqs. (20) and (21) for the liquid velocity field enable us to introduce the potential function of the flow:

$$div(\vec{V}) = 0 \qquad \text{in } D(t) \tag{20}$$

$$\overrightarrow{rot}(\vec{V}) = \vec{0} \qquad \text{in } D(t) \tag{21}$$

Indeed, if $\vec{V}$ is a non-null velocity field, the Eq. (21) is verified if and only if

$$\vec{V}(x, z, t) = \overrightarrow{grad}\,\phi(x, z, t) = \left(\frac{\partial\phi}{\partial x}(t), \frac{\partial\phi}{\partial z}(t)\right) \qquad \text{in } D(t) \tag{22}$$

with $\phi(x, z, t)$ the velocities potential of the fluid.

The velocity field is derived from the velocity potential $\phi(x, t)$ that verifies Laplace's Eq. (23) given by the previous relations (20) and (22).

$$\Delta\phi = 0 \qquad \text{in } D(t) \tag{23}$$

The general asymptotic expansion (19) of the velocity potential ϕ is introduced in the Eq. (23): the following development, $\phi(x, z, t) = \phi^{(0)} + \varepsilon \cdot \phi^{(1)} + O(\varepsilon)$, gives the Eq. (24), which is Laplace's equation at the first order.

$$\Delta\phi^{(1)} = 0 \qquad \text{in } D(t) \tag{24}$$

The free surface equation is $F(x, z, t) = 0$ for $x \in [0, b]$. Since free surface is a material boundary, the particle derivative can be applied to the previous equation to yield the following relation:

$$\frac{dF(x, z, t)}{dt} = \frac{\partial F}{\partial t} + \frac{\partial F}{\partial x}\frac{dx}{dt} + \frac{\partial F}{\partial z}\frac{dz}{dt} = 0 \tag{25}$$

If $\vec{U}(dx/dt, dz/dt)$ is the velocity field of fluid boundaries, the kinematic condition, $(\vec{U} - \vec{V}) \cdot \vec{n} = 0$, where $\vec{n} = \overrightarrow{grad}\,F / |\overrightarrow{grad}\,F|$ is the normal at the boundary, leads to the Eq. (26):

$$\frac{dF(x, z, t)}{dt} = \frac{\partial F}{\partial t} + \frac{\partial F}{\partial x}\frac{\partial \phi}{\partial x} + \frac{\partial F}{\partial z}\frac{\partial \phi}{\partial z} = 0 \qquad \text{on } SL(t) \tag{26}$$

If $n(x, t)$ represents the free surface elevation,

$$F(x, z, t) = n(x, t) - z = 0 \qquad \text{on } SL(t) \tag{27}$$

This latter equation instead of $F(x, z, t)$ in (26) gives the Eq. (28) that is expanded with the asymptotic development of free surface z-displacement (see Eq. (29)) to obtain the equation of first order (30). To be more precise, the kinematic Eq. (26) becomes the following relation:

$$\frac{\partial F}{\partial t} + \frac{\partial(n(x, t) - z)}{\partial x}\frac{\partial \phi}{\partial x} + \frac{\partial(n(x, t) - z)}{\partial z}\frac{\partial \phi}{\partial z} = 0 \qquad \text{on } SL(t) \tag{28}$$

As the free surface motion is assumed to be very small, the general form (19) of $n(x, t)$ leads to the Eq. (29) in which the higher term is of the first order:

$$n(x, t) = \varepsilon \cdot n^{(1)} + O(\varepsilon) \tag{29}$$

The Eq. (29) included in (28) gives the following relation:

$$\frac{\partial n^{(1)}}{\partial t} - \frac{\partial \phi^{(1)}}{\partial z} = 0 \qquad \text{on } SL(t) \tag{30}$$

The asymptotic expansion of the free surface dynamic condition must be led to solve the problem. In order to obtain this condition, Bernoulli's equation that establishes a relation between the velocities potential and the pressure of fluid P is given by the Eq. (31).

$$\frac{\partial \phi}{\partial t} + \frac{1}{2}\left|\overrightarrow{grad}\,(\phi)\right|^2 + \frac{P}{\rho} + g \cdot z = C(t) \qquad \text{in } D(t) \tag{31}$$

where ρ is the mass density, g the gravity and $C(t)$ is any function of time.

On the free surface, the fluid pressure is assumed to be equal to the atmospheric pressure Po. Using the form (19) for the physical variables of the Eq. (31) leads to the form of first order of Bernoulli's equation:

$$\frac{Po}{\rho} + \varepsilon \cdot \left(\frac{\partial \phi^{(1)}}{\partial t} + g \cdot n^{(1)}\right) + O(\varepsilon) = C(t) \qquad \text{on } SL(t) \tag{32}$$

The function $C(t)$ can be chosen equal to Po/ρ. The previous equation becomes of the first order:

$$\frac{\partial \phi^{(1)}}{\partial t} + g \cdot n^{(1)} = 0 \qquad \text{on } SL(t) \tag{33}$$

Then $n^{(1)}$ can be cancelled between the Eq. (33) and the Eq. (30) to yield the resultant condition that is an equation with the velocities potential only:

$$\frac{\partial^2 \phi^{(1)}}{\partial t^2} + g \cdot \frac{\partial \phi^{(1)}}{\partial z} = 0 \qquad \text{on } SL(t) \tag{34}$$

Three kinematic boundary conditions at the tank frontiers make up the problem. Sliding conditions are imposed on the lateral walls and on the ground. Therefore, the normal velocities on these frontiers are vanished:

$$
\begin{cases}
v(x = 0) = \dfrac{\partial \phi}{\partial x}(x = 0) = 0 \\[2mm]
v(x = b) = \dfrac{\partial \phi}{\partial x}(x = b) = 0 \qquad \text{on } SL(t) \\[2mm]
w(z = -h) = \dfrac{\partial \phi}{\partial z}(z = -h) = 0
\end{cases}
\tag{35a}
$$

The introduction of the asymptotic expansion of the velocity potential, $\phi(x, z, t) = \phi^{(0)} + \varepsilon \cdot \phi^{(1)} + O(\varepsilon)$, in the previous equations leads to boundary conditions that take the following form of the first order:

$$
\begin{cases}
\dfrac{\partial \phi^{(1)}}{\partial x}(x = 0) = 0 \\[2mm]
\dfrac{\partial \phi^{(1)}}{\partial x}(x = b) = 0 \qquad \text{on } SL(t) \\[2mm]
\dfrac{\partial \phi^{(1)}}{\partial z}(z = -h) = 0
\end{cases}
\tag{35b}
$$

The sloshing problem in a bidimensional tank carried out to the first order sums up the linearized eq uations governing the fluid motion:

$$
\frac{\partial^2 \phi^{(1)}}{\partial t^2} + g \cdot \frac{\partial \phi^{(1)}}{\partial z} = 0 \qquad \text{in } D(t)
\tag{36}
$$

$$
\Delta \phi^{(1)} = 0 \qquad \text{in } D(t)
\tag{37}
$$

$$
\frac{\partial \phi^{(1)}}{\partial x}(x = 0) = 0 \qquad \text{on } SL(t)
\tag{38}
$$

$$
\frac{\partial \phi^{(1)}}{\partial x}(x = b) = 0 \qquad \text{on } SL(t)
\tag{39}
$$

$$
\frac{\partial \phi^{(1)}}{\partial z}(z = -h) = 0 \qquad \text{on } SL(t)
\tag{40}
$$

Since the natural frequencies of this problem are the aim of this paragraph, the solution is assumed to be harmonic with a pulsation ω: $\phi^{(1)} = \varphi(x, z) \cdot e^{-i\omega t}$. This mathematical definition of the velocity potential is introduced in the previous equations. The Eqs. (36) to (40) of the problem become:

$$\frac{\partial \varphi}{\partial z} - \frac{\omega^2}{g} \cdot \varphi = 0 \qquad \text{in } D(t) \tag{41}$$

$$\Delta \varphi = 0 \qquad \text{in } D(t) \tag{42}$$

$$\frac{\partial \varphi}{\partial x}(x = 0) = 0 \qquad \text{on } SL(t) \tag{43}$$

$$\frac{\partial \varphi}{\partial x}(x = b) = 0 \qquad \text{on } SL(t) \tag{44}$$

$$\frac{\partial \varphi}{\partial z}(z = -h) = 0 \qquad \text{on } SL(t) \tag{45}$$

In order to solve the equations, the separation of variables x and z for function φ is assumed:

$$\varphi(x, z) = p(x) \cdot q(z) \tag{46}$$

Substituting this expression in Laplace's Eq. (42) results in two distinct equations, in which the parameter k, a constant value, is the wave number:

$$\frac{\partial^2 p}{\partial x^2} + k \cdot p = 0 \tag{47}$$

$$\frac{\partial^2 q}{\partial z^2} - k \cdot q = 0 \tag{48}$$

The expressions (49) and (50) give the well-known solutions of Eqs. (47) and (48), which are substituted in the boundary conditions through the velocity potential.

$$p(x) = A \cdot \cos(k \cdot x) + B \cdot \sin(k \cdot x) \tag{49}$$

$$q(z) = C \cdot ch[k \cdot (z + h)] \tag{50}$$

where A, B and C are constant values.

The function $q(z)$ is defined in order to satisfy the boundary condition (45).

By using the definition (46) of the function $\varphi(x, z)$, the Eqs. (49) and (50) are then inserted in the Eqs. (43) and (44). After simplifications, we obtain respectively:

$$B = 0 \tag{51}$$

$$A \cdot \sin(k \cdot b) = 0 \tag{52}$$

This last equation involves the following relation, in which n is an integer number:

$$k \cdot b = n \cdot \pi \tag{53}$$

Similarly, the dynamic free surface condition (41) becomes the well-known dispersion relation between the pulsation ω and the wave number k, (Wiegel):

$$\omega^2 = g \cdot k \cdot th(k \cdot h) \tag{54}$$

As the pulsation is defined by: $\omega = 2 \cdot \pi \cdot f$, the Eqs. (53) and (54) give the slosh frequency f, (Blevins 1995)*:*

$$f = \frac{1}{2}\sqrt{\frac{g \cdot n}{b\pi}th\left(\frac{n\pi h}{b}\right)} \quad \text{with } n, \text{ an integer number} \tag{55}$$

Two extreme cases can be studied in order to understand the physical meaning of the formula (55): the basin depth is smaller than the breadth or, conversely, the depth of the tank is bigger than the breadth. In the shallow liquid case, h is smaller than b. Therefore, the fundamental natural frequency is estimated by the following equation:

$$f_0 = \frac{\sqrt{gh}}{2b} \quad \text{if} \quad \frac{h}{b} < \frac{1}{10} \tag{56}$$

The resonance frequency of surface waves in a harmonic rolling tank with large lateral dimension appears as the wavelength λ equals twice the breadth b and the celerity equals the gravity wave velocity: $\lambda_0 = 2b$ and $c_0 = \sqrt{g \cdot h}$. For a lake whose the breadth is of order of kilometers, the natural period is of the order of minutes or even hours.

In the deep liquid case, h is higher than b. The fundamental frequency is approximated by the following expression:

$$f_0 = \frac{1}{2}\sqrt{\frac{g}{\pi b}} = \frac{\sqrt{\frac{gb}{\pi}}}{2b} \quad \text{if} \quad \frac{h}{b} > 1 \tag{57}$$

The resonance frequency of surface waves in a harmonic rolling tank with large lateral dimension appears as the wavelength λ equals twice the breadth b and the celerity equals a particular gravity wave velocity: $\lambda_0 = 2b$ and $c_0 = \sqrt{\frac{g \cdot b}{\pi}}$. In both particular cases, the fundamental natural frequency of a basin decreases with increasing tank breadth.

7. Numerical results

To validate the numerical model, Eq. (55) is used to predict sloshing frequencies for a simple tank with various fuel amounts. The tank chosen was approximately 100 inches (254 cm) by 50 inches (127 cm). Three different fuel heights were analyzed: 25%, 50% and 75%.

Next, this specific tank was modeled by a mesh composed of 17988 solid elements and a sloshing event was introduced. Initially assigning velocities to both the tank and the fluid, then stopping the tank motion at 0.00001 seconds created the sloshing event. Rigid material was used to represent tank walls. The finite element model and the induced sloshing event are shown in Fig. 6.

Comparing the predicted sloshing frequencies against calculated values for three different fuel levels reveals a maximum error below 3%, see Fig. 7. This analysis demonstrates that LS-DYNA can accurately predict sloshing frequencies.

Now that the analysis method has been validated, the effects of baffles on sloshing frequency were investigated. Three different baffle configurations were investigated, see Fig. 8.
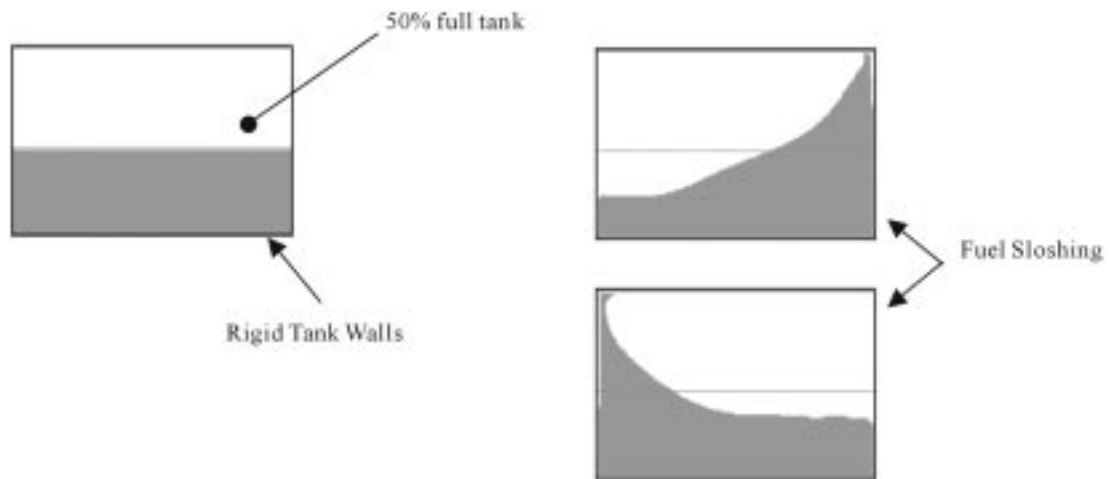
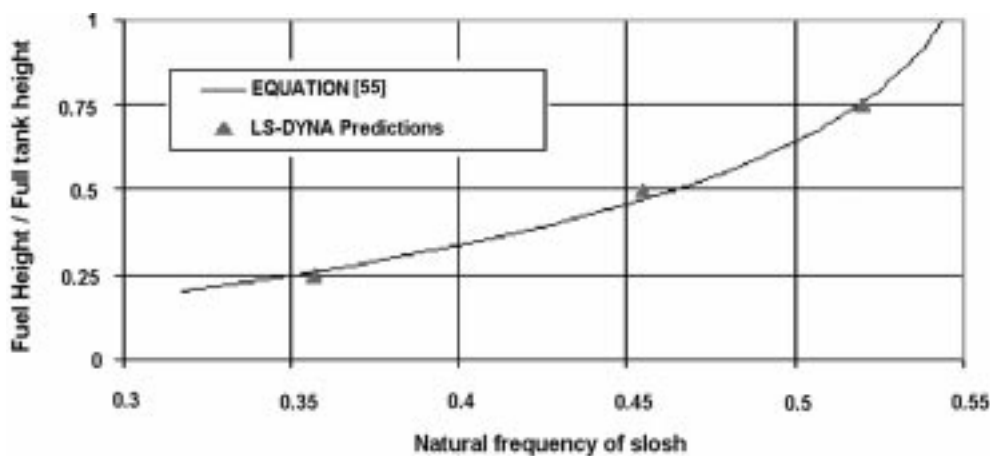Fig. 6 Finite element model and analysis depicting a sloshing event

Fig. 7 Plot comparing calculated and predicted sloshing frequencies for a sample tank without baffles

Comparing the predicted sloshing frequencies reveals some interesting results, see Fig. 9. Notice that case 1, baffles without holes, behaves like an under damped system. Case 2, baffles with small holes, behaves like a damped system, and case 3, baffles with large holes, behaves like a critically damped system.

This behaviour is directly related to the flow through the baffles. Specifically, vortices are created as flow travels between the adjacent bays, see Fig. 10. These vortices consume energy, thus reducing the overall energy in the problem. Fig. 10 shows the flow through the baffles, which damps out the fluid forces applied on the structure.
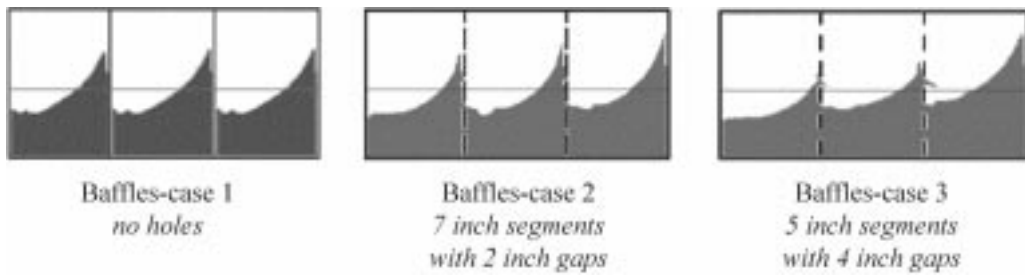
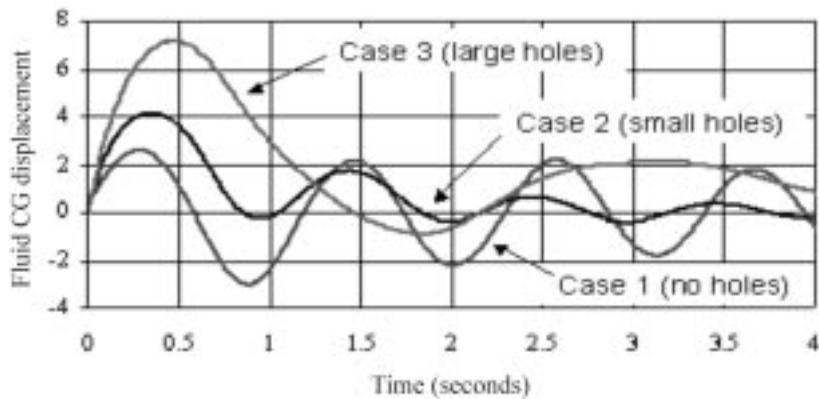Fig. 8 Half filled tank in three different baffle configurations

Fig. 9 Displacement of the center of gravity of the fluid versus time for three cases: no holes, small holes, large holes
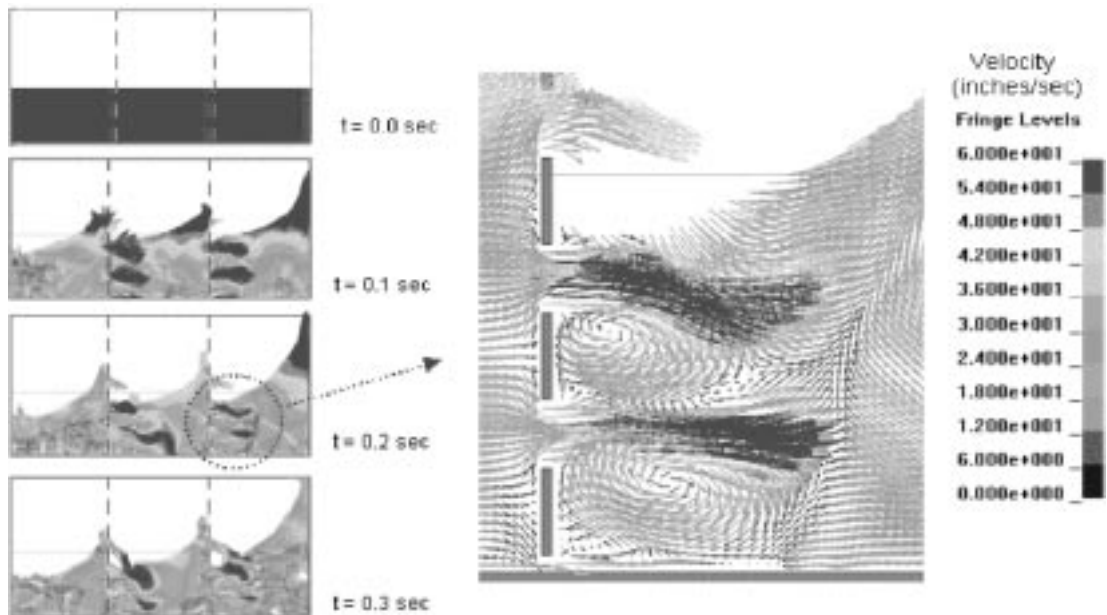

Fig. 10 Time history 'snap-shots' showing fluid flow

References

Amsden, A.A. and Hirt, C.W. (1973), "YAQUI: An arbitrary Lagrangian-Eulerian computer program for fluid flow at all speeds", Los Alamos Scientific Laboratory, LA-5100.

Benson, D.J. (1992), "Computational methods in Lagrangian and Eulerian hydrocodes", *Comput. Methods Appl. Mech. Eng.*, **99**, 235-394.

Benson, D.J. (1992), "Momentum advection on a staggered mesh", *J. of Computational Physics*, **100**(1), May 1992, 143-162.

Benson, D.J. (1997), "A mixture theory for contact in multi-material Eulerian formulations", *Comput. Methods Appl. Mech. Eng*. **140**, 59-86.

Benson, David J. (1998), "Eulerian finite element methods for the micromechanics of heterogenous materials: Dynamics prioritization of material interfaces", *Comput. Meth. Appl. Mech. Eng.*, **150**, 343-360.

Blevins, R. (1995), *Formulas for Natural Frequency & Mode Shape*, Frieger Publishing Corporation.

Flanagan, D.P. and Belytschko, T. (1981), "A uniform strain hexahedron and quadrilateral and orthogonal hourglass control", *Int. J. Numer. Meths, Eng.*, **17**, 679-706.

Hallquist, J.O. (1998), "LS-DYNA theoretical manual", Livermore Software Technology Company.

Hughes, T.J.R., Liu, W.K. and Zimmerman, T.K. (1981), "Lagrangian Eulerian finite element formulation for viscous flows", *J. Comput. Methods Appl. Mech. Engrg.*, **21**, 329-349.

Lee, S.-Y., Cho, J.-R., Park, T.-H. and Lee, W.-Y. (2002), "Baffled fuel-storage container: Parametric study on transient dynamic characteristics", *Struct. Eng. Mech., An Int. J.*, **13**(6), 653-670.

Nakayama, T. and Mori, M. (1996), "An Eulerian Finite Element method for time-dependent free-surface problems in hydrodynamics", *Int. J. Numer. Methods in Fluids*, **22**(3), 175-194.

Richtmyer, R.D. and Morton, K.W. (1967), *Difference Equations for Initial-Value Problems*, Interscience Publishers, New York.

Souli, M. and Zolesio, J.P. (2001), "Arbitrary Lagrangian-Eulerian and free surface methods in fluid mechanics", *Comput. Methods Appl. Mech. Eng.,* **191**.

Souli, M., Ouahsine, A. and Lewin, L. (2000), "ALE formulation for fluid-structure interaction problems", *Comput. Methods Appl. Mech. Eng.*, **190**, 659-675.

Summit Racing Equipment, Akron, Ohio 44309.

Van Leer, B. (1977), "Towards the ultimate conservative difference scheme. IV. A new approach to numerical convection", *J. of Computational Physics*, **23**, 276-299.

Wiegel, L.R., *Oceanographical Engineering*, Prentice hall Inc Publisher.

Woodward, P.R. and Collela, P. (1982), "The numerical simulation of two-dimensional fluid flow with strong shocks", Lawrence Livermore National Laboratory, UCRL-86952.

Young, D.L. (1982),"Time-dependent multi-material flow with large fluid distortion", *Numerical Methods for Fluids Dynamics*, Ed. Morton, K.W. and Baines, M.J., Academic Press, New-York.